

# Unbroadened-spectrum chirped modulation: on the relation between chirp induction mechanism and spectral broadening

Paolo Bravetti, Stefano Balsamo, Jorge Alberto Villa Montoya are with Avanex Corporation, Via F. Fellini 4, 20097 San Donato Milanese (MI), Italy. R. Brouard and V. Rouffange are with APEX Technologies, 7 rue Soddy, 94000 Créteil (France)

**Abstract**—The spectrum of a chirped optical NRZ data stream obtained by an external Mach-Zehnder Modulator (MZM) is analyzed. We demonstrate that it is possible to induce chirp without broadening the optical spectrum by employing a MZM with optical power unbalancing in the two waveguides, such as the one discussed in [4]. For standard chirped MZM (different electrical field on the two arms), such as z-cut LiNbO<sub>3</sub> modulators, the broadening as a function of chirp factor is measured for comparison.

**Index Terms**—External modulator, chirp parameter, power spectrum, Mach-Zehnder modulators, time-resolved chirp, tunable chirp.

## I. INTRODUCTION

SPECTRAL density of optical signals is an important parameter to consider in the design of high capacity fiber transmission systems. In particular, maximizing the information spectral density allows cost reduction of installed systems, one of the strongest needs of today's telecom community. Optical duobinary, for example, has been extensively studied also because of its high spectral efficiency [1,2]. On the other hand, it is widely recognized that chirped modulation formats, such as chirped Non Return to Zero (NRZ) on-off keying, have lower spectral density, due to spectrum broadening induced by chirp itself [3]. Chirp effect on spectral density has been studied analytically in a recent work [3], which also underlines the interaction between chirp and rise-fall times.

We recently investigated chirp properties of Mach-Zehnder Modulators (MZM) and their relation with the method used to induce chirp [4]. In the aforementioned paper, we pointed out differences in Time Resolved Chirp (TRC) shape and transmission properties of 10 Gb/s NRZ signals, due to the chirp inducing mechanism.

chirped MZM for NRZ modulation format. We demonstrate that the spectral density depends not only on the chirp factor, but on the chirping method as well: we show for the first time that our method for chirp induction, besides being very effective for transmission, doesn't broaden the power spectrum with respect to a zero chirp device.

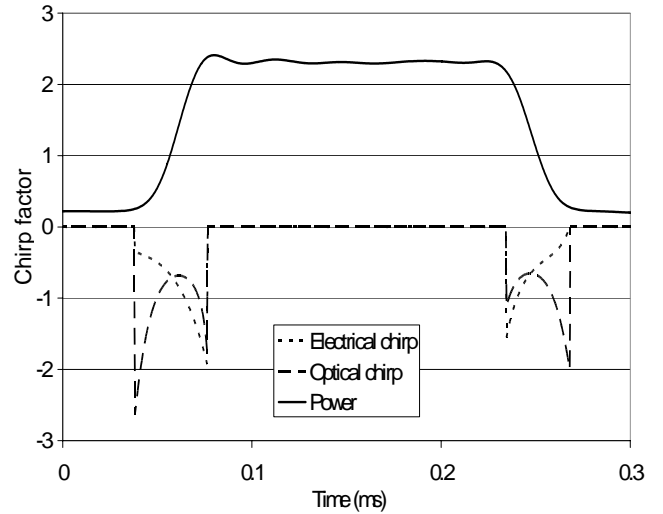


Fig. 1. Time resolved chirp measurement: electrical chirp (dotted line), optical chirp (dashed line) and pulse power (solid line).

In this paper we investigate the spectral properties of

## II. BACKGROUND: CHIRP MECHANISM

Frequency chirping can be generated by either inducing asymmetry in electrical to optical conversion efficiency (i.e. unbalancing the electric field “seen” by the two waveguides of a MZM) or modifying the optical power ratio between the two MZM arms (we will refer, hereafter, to these two chirp factors as “electrical chirp” and “optical chirp”, respectively). In recent times, we proposed a new kind of LiNbO<sub>3</sub> MZM with widely tunable optical chirp using a simple DC voltage on one port [5,6]. We also studied the differences between the two kinds of chirp [4]. In particular we showed that TRC chirp varies with time linearly for electrical chirp and quadratically for optical chirp. Figure 1 shows new high definition measurements, performed with a pulse-chirp-spectrum analyzer employing interferometer techniques (see §IV), which compare TRC of the two chirp mechanisms. Moreover, in [4] we pointed out the different dependence of transmission performances on driving voltage and extinction ratio, showing the improvement that optical chirp gives over electrical one.

## III. EXPERIMENTS

We experimentally characterized both electrical and optical chirp in terms of power spectrum. For optical chirp we used a single MZM with tunable chirp [5, 6], at four different chirp values (small-signal chirp factor [7]: -0.7, -0.52, -0.35 and -0.18), while for electrical chirp we employed three distinct modulators with different chirp values (small-signal chirp factor was -0.4, -0.5 and -0.7) and same bandwidth. As a zero-chirp reference modulator we used the tunable chirp modulator on the zero point of its chirp versus voltage characteristic. At transmitter side the set-up was composed by a PRBS Pulse Pattern Generator (PPG), a wideband modulator driver, a tunable laser at 1550 nm, and the MZMs. The transmitted signal power was then split, one part of the radiation being analyzed by a monochromator-based Optical Spectrum Analyzer (OSA) with 0.01 nm resolution and the remaining part being sent into an oscilloscope to control extinction ratio and crossing point. For the high resolution measurements we used the same instrument employed for chirp analysis, instead of the conventional OSA (see §IV). We acquired the power spectrum of the transmitted signal while varying several parameters, namely, the chirp (involving a change of the whole modulator for electrical chirp), the driving voltage amplitude and crossing point of the optical eye diagram (by changing the MZM bias point). Since the optical power spectrum depends on all these parameters, we chose to study each one of the different factors.

First of all, we studied chirp factor dependency: Figure 2 reports the spectral broadening as a function of the chirp factor, for both electrical and optical chirp. The spectral width was calculated by fitting with a polynomial interpolator the main lobe of the optical PRBS spectrum at transmitter output.

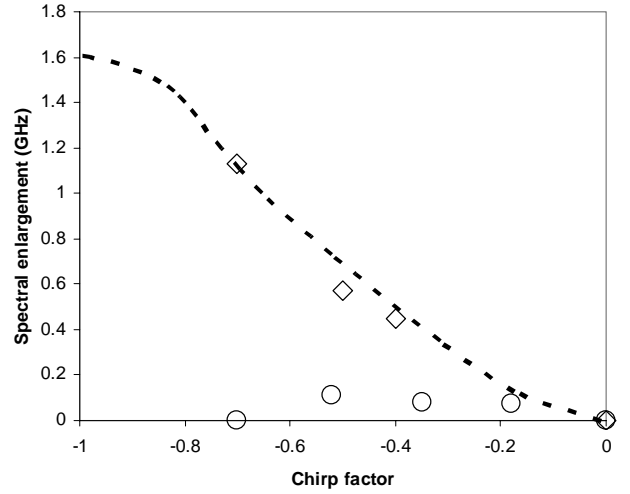


Fig. 2. Spectral broadening due to chirping in NRZ electrically chirped modulators: simulation (dashed line) and measurements (diamonds) are in very good agreement. Circles represent spectral width measurements on optically chirped MZM.

Then, the width at -20 dB from the top of the lobe (without considering the optical carrier) was calculated. Zero chirp condition was taken as the reference value. We can see a significant broadening in case of electrical chirp, around 1.1 GHz at -0.7 chirp factor (the total width at -20 dB from the top is of the order of 20 GHz) and no broadening at all for optical chirp. The figure also shows the theoretical curve obtained through computer simulation: the agreement between calculations and measurements is very good.

In order to investigate in depth the case of optical chirp, we also performed high resolution spectrum measurements. Figure 3 shows the power spectrum for a 2<sup>31</sup>-1 PRBS sequence with 100 MHz resolution, confirming that no broadening at all is noticeable for the optical chirp.

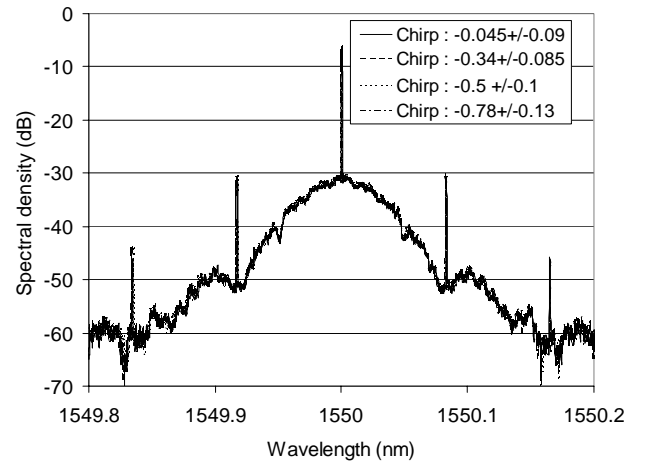


Fig. 3. Power spectrum of optically chirped (tunable) MZM at different chirp values: the spectrum doesn't change with chirp

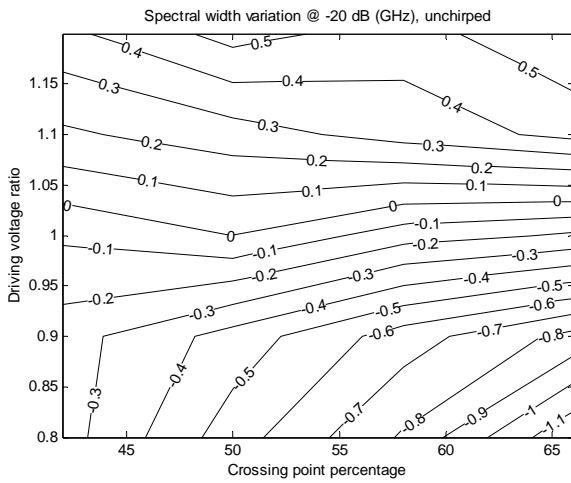


Fig. 4. Unchirped MZM: variation of spectral width at -20 dB for different driving voltages and crossing points.

The effect of changing the driving voltage and the crossing point on an unchirped device is shown in figure 4. Driving voltage is reported as the fraction of the voltage needed to reach the maximum dynamic extinction ratio (DER) on the transmitted eye pattern. Variations of spectral width are calculated with respect to the case of 50% crossing and driving voltage corresponding to maximum DER. From the graph we can see that a higher driving voltage yields a wider spectrum, while the effect of crossing is noticeable only at low or high driving voltages. Crossing dependence of spectral width doesn't change when chirp (electrical or optical) is present. The driving voltage, instead, plays a different role depending on the chirp type: comparing figures 5a and 5b we can see that the spectral broadening is higher for electrical chirp, and has more effect at higher chirp values. From figure 5 we also have a clear picture of the different spectral width dependence on chirp for electrical and optical chirp, no broadening being present in this latter case.

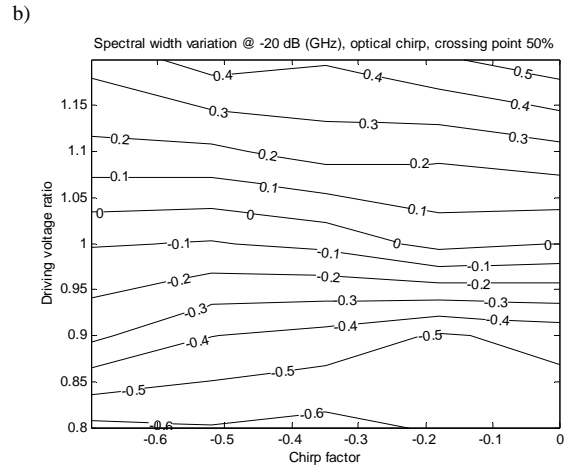
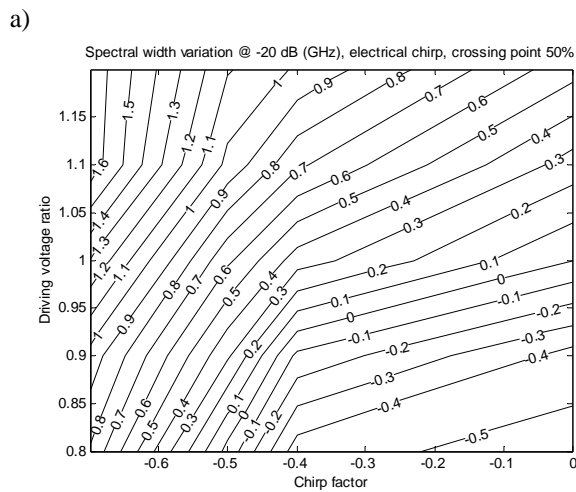
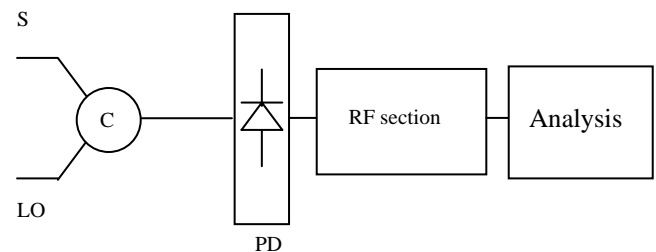


Fig. 5. Spectral enlargement at -20 dB due to chirp factor and driving voltage for electrical (a) and optical (b) chirp.

#### IV. PRINCIPLES OF HIGH RESOLUTION SPECTRAL ANALYSIS AND TIME-RESOLVED CHIRP ANALYSIS

The high resolution spectral analysis is performed by an heterodyne detection technique (see figure 6). The optical signal under test (S) is mixed through an optical combiner with a tunable laser, acting as a local oscillator (LO). At the output of the coupler, the interference of the two optical fields results in beating of the optical power, and the beat spectrum corresponds to a mathematical convolution of the input fields spectra ([8]). By photodetection, the beating optical power is converted into electrical signal which is then filtered by the RF section. By tuning the LO over an appropriate spectral range, the spectrum can be measured with 100 MHz resolution or 20MHz.



S = optical signal under test  
 LO = local oscillator laser (tunable)  
 C = optical combiner  
 PD = photodetector

Fig. 6. Schematic description of the setup for the high resolution spectrum analysis, based on heterodyne detection.

The time-resolved chirp analysis of a periodic optical signal is obtained by a Fourier transform of its complex spectrum (the complex spectrum means the power and phase values of all the spectral components). The power spectrum, which is composed of several lines equally spaced by the inverse of the time period (frequency  $F$ ), is measured with the heterodyne technique described above, and the relative optical phases of all these lines are measured with the following technique ([10]). The intensity of the optical signal under test (see figure 7) is modulated through a Mach-Zehnder modulator (MZM), driven by a time varying sinusoidal electrical signal at frequency  $F/2$ .

PPG = Pulse Pattern Generator  
 MZM = Mach Zehnder Modulator under test  
 MZM2 = MZM used for chirp measurement  
 Freq. div. = frequency divider  
 $\tau$  = time delay

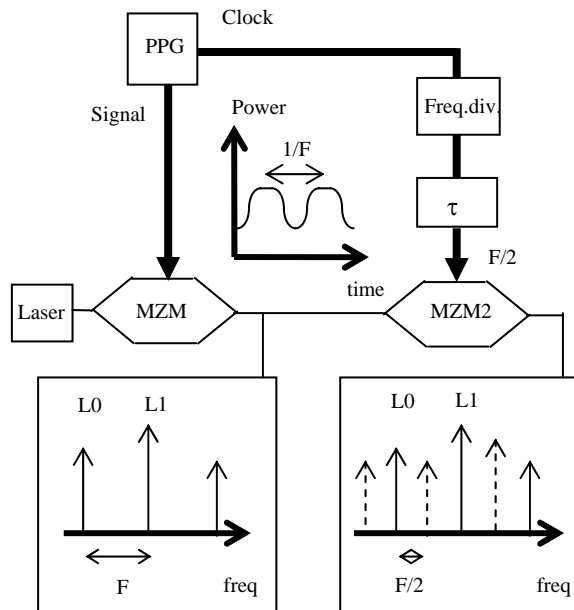


Fig. 7. Schematic description of the setup used for chirp measurement.

Each original spectral line at frequency  $F_0$  generates in the transmitted spectrum two new spectral lines at frequency  $F_0 \pm F/2$ . Neighbouring lines  $L_0$  and  $L_1$ , located at frequencies  $F_0$  and  $F_0 + F$ , generate in particular two lines coinciding at their middle frequency  $F_0 + F/2$ , thus giving a single new line whose optical power results from the interference between these two coinciding lines. It is proportional to  $\cos(2\pi F\tau + \Delta\Phi)$ , where  $\Delta\Phi$  is the optical phase difference between  $L_0$  and  $L_1$ , and  $\tau$  is the time delay applied to the modulating electrical signal with respect to the optical signal under test.  $\Delta\Phi$  can be retrieved (and thus the relative phases of all the spectral lines) by measuring this power as a function of  $\tau$ , which is done by analysing the transmitted spectrum

(employing the same heterodyne technique) for different values of  $\tau$ .

After measuring the full complex spectrum with this method, one calculates the amplitude and phase of the optical field in the time domain by Fourier transform (over one period), giving time-resolved power and chirp factor, like shown on figure 1.

## V. CONCLUSION

We demonstrated that the chirp induced by unbalancing the optical power in the two arms of a MZM doesn't produce spectral broadening of the transmitted spectrum. For standard chirped (i.e. electrical field unbalanced) MZM we found a broadening of about 1.1 GHz at -20 dB for a chirp factor of -0.7, in perfect agreement with simulation.

## REFERENCES

- [1] Y. Yano, T. Ono, K. Fukuchi, T. Ito, H. Yamazaki, M. Yamaguchi, and K. Emura, "2.6 Terabit/s WDM transmission experiment using optical duobinary coding," *ECOC 1996*, paper ThB.3.1
- [2] P. Bravetti, L. Möller, G. Ghislotti, C. Cavalli, C. Gualandi, P. Bergamini, "Impact of Response Flatness on Duobinary Transmission Performance: An Optimized Transmitter With Improved Sensitivity", *IEEE Phot. Tech. Lett.*, vol. 16, n. 9, Sep. 2004.
- [3] Keang-Po Ho, and Joseph M. Kahn, "Spectrum of Externally Modulated Optical Signals", *IEEE J. Light. Tech.*, vol. 22, n. 2, Feb. 2004, pp. 658-663.
- [4] P. Bravetti, G. Ghislotti, S. Balsamo, "Chirp inducing mechanisms in Mach-Zehnder modulators and their effect on 10 Gb/s NRZ transmission studied using tunable-chirp single drive devices", *IEEE J. Light. Tech.*, vol. 22, n. 2, Feb. 2004, pp. 605-611.
- [5] S. Balsamo, P. Bravetti, G. Ghislotti, "Single-drive LiNbO3 Mach-Zehnder modulator with widely DC tunable chirp", in *Eur. Conf. Optical Communication (ECOC 2002), Rimini, Italy, Paper Mo 4.5.3*
- [6] G. Ghislotti, S. Balsamo, P. Bravetti, "Single-drive LiNbO3 Mach-Zehnder modulator with widely DC tunable chirp", *IEEE Phot. Tech. Lett.*, vol. , n. , Sep. 200
- [7] F. Devaux, Y. Sorel, and J. F. Kerdiles, "Simple measurement of fiber dispersion and of chirp parameter of intensity modulated light emitter", *IEEE J. Light. Tech.*, vol. 11, n. 12, pp. 1937-1940 (1993)
- [8] D. M. Baney, W. V. Sorin, "High resolution optical frequency analysis", in D. Derickson, *Fiber optic test and measurement*, Prentice Hall, Hewlett-Packard professional book, chap. 5, pp. 169-219 (1998)
- [9] S. B. Alexander, "Design of wide-band optical heterodyne balanced mixer receivers", *IEEE J. Light. Tech.*, vol. LT-5, n. 4, pp. 523-537 (1987)
- [10] J. Debeau, B. Kowalski, R. Boittin, "Simple method for the complete characterization of the optical pulse", *Optics Letters*, vol. 23, n. 22, pp. 1784-1786 (1998)